

Cosmic Dust

The Ulysses perspective

Eberhard Grün¹, Harald Krüger¹, Markus Landgraf²

1: Max-Planck-Institut für Kernphysik, Postfach 10 39 80, 69029 Heidelberg, Germany

2: ESA-ESOC, Robert-Bosch-Str. 5, 64293 Darmstadt, Germany

To appear in: **The heliosphere at solar minimum: The Ulysses perspective**,
eds. A. Balogh, R. Marsden, E. Smith; Springer Praxis, 2001

Chapter 9

Cosmic Dust

By *Eberhard Grün*¹, *Harald Krüger*¹, *Markus Landgraf*²

1: Max-Planck-Institut für Kernphysik, Postfach 10 39 80, 69029 Heidelberg, Germany

2: ESA-ESOC, Robert-Bosch-Str. 5, 64293 Darmstadt, Germany

9.1 Introduction

There are several methods to study cosmic dust. The traditional method to determine the global structure of the interplanetary dust cloud is by zodiacal light observations (for a review see, e.g. [55]). Before Ulysses, zodiacal light observations have provided the primary means of studying the out-of-ecliptic distribution of the interplanetary dust cloud. By inversion of these scattered light observations it has been derived that the grain properties depend upon their elevation above the ecliptic plane, i.e. upon the inclination of their orbits [59]. Several 3-dimensional models of the intensity, polarization and color of the zodiacal dust cloud have been developed [14, 15].

Thermal infrared observations by IRAS [36] and especially COBE [65] give further constraints on the zodiacal dust cloud outside and above the Earth's orbit. Interpretations of these observations, however, rely heavily on assumptions about the size distribution and material properties of the dust particles. More recently, the infrared spectral energy distribution and brightness fluctuations in the zodiacal cloud have been studied with ISO [1, 2]. These observations will also allow for a better determination of the size distribution of the interplanetary dust grains.

The dust experiments on board the Pioneer 10 and Pioneer 11 spacecraft provided information on the radial dependence of the spatial density of large dust grains ($\sim 20 \mu\text{m}$ diameter) outside Earth's orbit. Between 1 and 3.3 AU these experiments detected a decrease of the dust abundance proportional to $r^{-1.5}$, r being the heliocentric distance [43, 35]. The photometer on board Pioneer 10 did not record any scattered sunlight above the background beyond the asteroid belt while the penetration experiment recorded dust impacts out to about 18 AU heliocentric distance at an almost constant rate [44].

Measurements of dust in the inner solar system with the Pioneer 8, Pioneer 9 and Helios space probes and the HEOS 2 satellite showed that there are several populations of dust particles which possess different dynamical properties. A population of slow-moving, small ($10^{-16} \text{ kg} < m < 10^{-14} \text{ kg}$) particles has been observed by the Pioneer 8/9 [8] and HEOS 2 [38] dust experiments. The Helios dust experiment [17] confirmed these particles which orbit the Sun on low eccentric orbits ($e < 0.4$). These low angular momentum “apex” particles were thought to originate from collisional break-up of larger meteoroids in the inner solar system [18]. Another population which consists of very small particles ($m \sim 10^{-16} \text{ kg}$) has been detected by the Pioneer 8/9 and Helios space probes arriving at the sensors from approximately the solar direction. These particles have been identified [73] as small grains generated in the inner solar system which leave the solar system on hyperbolic orbits due to the dominating effect of the radiation pressure force (β -meteoroids).

The orbital distribution of larger meteoroids is best known from meteor observations. Sporadic meteoroids move on orbits with an average eccentricity of 0.4 and an average semi-major axis of 1.25 AU at Earth’s orbit [67]. Helios measurements allowed the identification of an interplanetary dust population [17] which consists of particles on highly eccentric orbits ($e > 0.4$) and with semi-major axes larger than 0.5 AU. Pioneer 11 in-situ data obtained between 4 and 5 AU are best explained by meteoroids moving on highly eccentric orbits [44]. These particle populations resemble most closely the sporadic meteor population.

Before Ulysses, dust has been observed in the magnetosphere of Jupiter, both by in-situ experiments on board Pioneer 10 and Pioneer 11, and by remote sensing instrumentation on board Voyager 1 and Voyager 2. Pioneer 10/11 measured a 1000 times higher flux of micrometeoroids in the vicinity of Jupiter compared with the interplanetary flux. The Voyager imaging experiment detected a ring of particulates at distances out to 2.5 jovian radii, as well as volcanic activity on the jovian satellite Io.

One of the most important results of the Ulysses mission is the identification and characterization of a wide range of interstellar phenomena inside the solar system. A surprise was the identification and the dominance of the interstellar dust flux in the outer solar system. Before this discovery by Ulysses it was believed that interstellar grains are prevented from reaching the planetary region by electromagnetic interaction with the solar wind magnetic field. The interplanetary zodiacal dust flux was thought to dominate the near-ecliptic planetary region while at high ecliptic latitudes only a very low flux of dust released from long-period comets should be present. Therefore, the characterization of the interplanetary dust cloud was the prime goal of the Ulysses dust investigation.

Around Jupiter fly-by in 1992 Ulysses has discovered intense collimated streams of dust particles. The grains were detected at a distance out to 2 AU from Jupiter along the ecliptic plane and at high ecliptic latitudes [22]. Modelling of the dust trajectories showed that the grains must have been ejected from the jovian system [74]. Later measurements by the Galileo spacecraft within the jovian magnetosphere revealed Io

as the source of the grains [16].

Here, we focus on measurements by the in situ dust detectors on board the Ulysses and Galileo spacecraft to obtain information on the large scale structure and the dynamics of the interplanetary dust cloud (Section 9.3), dust in the environment of Jupiter (Section 9.4), and interstellar dust (Section 9.5). The dust detectors measure dust along the the spacecraft's interplanetary trajectories. From these measurements 3-dimensional model of the spatial dust distribution can be constructed. The orbits of the Galileo and Ulysses spacecraft are displayed in Fig. 9.1.

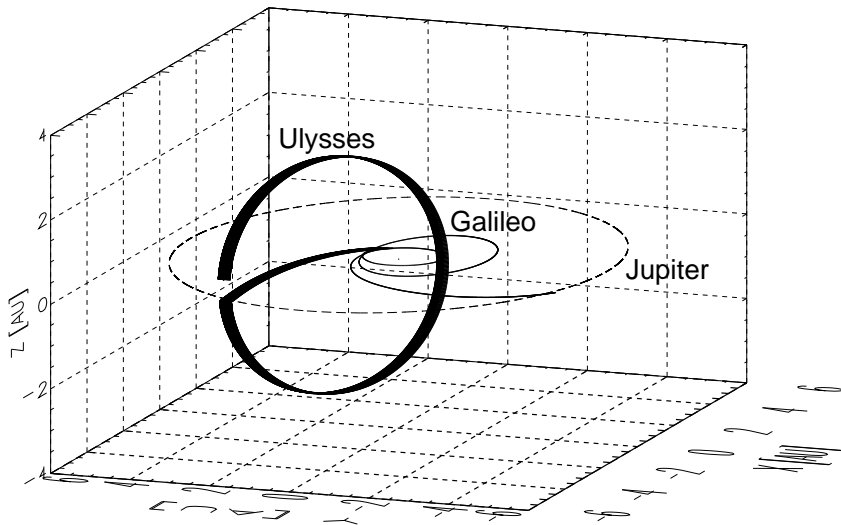


Figure 9.1: Trajectories of the Ulysses (heavy solid line) and the Galileo (thin solid line) spacecraft. The Sun is in the center, Jupiter's (dashed) and Galileo's trajectories are in the ecliptic plane. The initial trajectory of Ulysses from Earth to Jupiter was also in the ecliptic plane. Subsequently, Ulysses was thrown into an orbit plane inclined by 79° to the ecliptic plane. Vernal equinox is towards the positive x direction and north is at the top. The Ulysses trajectory is shown until the end of 1997.

9.1.1 Dust objectives

The Ulysses spacecraft was launched in October 1990 onto a direct trajectory to Jupiter. After Jupiter fly-by in February 1992, Ulysses was thrown onto an orbit of 79° inclination that passed close to the ecliptic poles. The passage from the south to the north pole took one year from September 1994 to September 1995 and the passage through the ecliptic plane occurred in March 1995. Ulysses completed a full polar orbit in April 1998 when it reached its aphelion distance at 5.4 AU again, however, this time Jupiter was on the opposite side of the Sun.

Ulysses carried a high sensitivity dust detector to the outer solar system for the first time. The detector is five orders of magnitude more sensitive than those on

the Pioneer 10 and Pioneer 11 spacecraft [44]. The objectives of the Ulysses dust experiment (as stated in the original proposal [21]) were to

- (1) determine the 3-dimensional structure of the zodiacal cloud,
- (2) characterize its dynamical state, and
- (3) search for interstellar dust penetrating the solar system.

The prime objective was the determination of the 3-dimensional dust distribution in the solar system. In order to reach this goal with the help of out-of-ecliptic Ulysses measurements, reference dust measurements had to be provided in the ecliptic plane. This was almost ideally achieved by the Galileo mission that was launched a year earlier but took dust measurements for 6 years in interplanetary space near the ecliptic plane with a twin of the Ulysses dust detector. While Ulysses data are very good at determining the absolute latitude dependence (and inclination dependence) of meteoroids, measurements by Galileo near the ecliptic plane determine the radial and eccentricity dependence for low inclination orbits. The achievement of the third Ulysses objective, namely, the identification of interstellar dust particles, required that interstellar dust had to be identified and separated from interplanetary dust. For measurements by both the Galileo and Ulysses detectors, this distinction was easy outside about 3 AU because it was found that the flux of interstellar dust grains dominated and differed significantly from prograde interplanetary dust, both in direction and speed [22, 24, 4, 5].

9.2 Instrumentation

Ulysses is a spinning spacecraft with its spin-axis being coincident with the antenna pointing direction. Its antenna usually points towards Earth. The Ulysses dust detector is mounted at an angle of 85° from the antenna direction. The field-of-view (FOV) of the dust detector is a cone of 140° full angle and the spin averaged effective sensor area for impacts varies with the angle between the impact direction and the antenna direction [21]. Because the detector is mounted almost perpendicular to the spacecraft spin-axis, the maximum spin-averaged sensitive area of 200 cm^2 is reached for impacts along a plane almost perpendicular to the antenna direction (the geometry of dust detection during Jupiter fly-by is sketched in Fig. 9.8). The impact direction (rotation angle, ROT) in this plane is determined by the spin position of the spacecraft around its spin-axis at the time of a dust impact. The rotation angle is zero when the dust sensor axis is closest to the ecliptic north direction. The rotation angle is measured in a right-handed system around the antenna direction.

The Ulysses dust detector [21] is an impact ionization sensor which measures the plasma cloud generated upon impact of submicrometer- and micrometer-sized dust particles onto the detector target (cf. Fig. 9.2). Up to 3 independent measurements of the ionization cloud created during impact are used to derive both the mass and

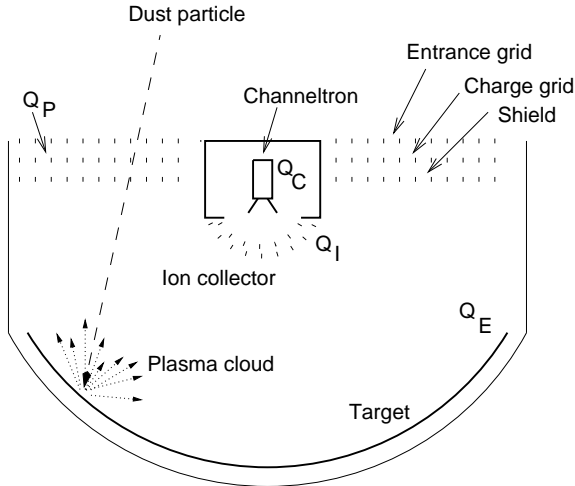


Figure 9.2: Schematic configuration of the Ulysses dust detector (GRU). Particles hitting the target create a plasma cloud and up to three charge signals (Q_I , Q_E , Q_C) are used for dust impact identification.

the impact speed of the dust grains [25]. The detector mass threshold, m_t , is proportional to the positive charge component, Q_I , of the plasma produced during the impact, which itself strongly depends on the impact speed, v . Using the calibration parameters $(Q_I/m)_0$, m_0 , v_0 , and α , which have been approximated from detector calibrations [25], the corresponding mass threshold can be calculated:

$$m_t = \frac{Q_I}{(Q_I/m)_0} = m_0 \left(\frac{v_0}{v} \right)^\alpha, \quad (9.1)$$

with $\alpha \sim 3.5$. For example, an impact charge of $Q_I = 8 \cdot 10^{-14}$ C refers to a mass threshold $m_t = 3 \cdot 10^{-17}$ kg at 20 km s^{-1} impact speed.

The dynamic range of the impact charge measurement is 10^6 which is also the dynamic range of the mass determination for particles with constant impact speeds. The calibrated speed range of the instrument is $2 \text{ km s}^{-1} \leq v \leq 70 \text{ km s}^{-1}$ which corresponds to a calibrated mass range of $10^{-19} \dots -9$ kg. Impact speeds can be determined with an accuracy of about a factor two and the accuracy of the mass determination of a single particle is about a factor of 10.

Impact-related data such as up to three charge measurements, impact time and rotation angle are normally all transmitted to Earth for each impact. Thus, a complete record of impact charge, particle mass, impact velocity, impact time and impact direction is available for each detected particle. Impact rates are derived from the number of detections within a given time interval.

In addition to Ulysses, the Galileo spacecraft carries a nearly identical dust detector on board. After being launched in 1989 Galileo traversed interplanetary space and was injected into a bound orbit about Jupiter in 1995. Galileo dust data supplement Ulysses measurements because Galileo measured dust along the ecliptic plane at times when Ulysses was at high ecliptic latitudes. This allowed for the determination of radial and latitudinal variations of the interplanetary dust cloud [29]. Dust data obtained with the detectors on board both spacecraft – Ulysses and Galileo – can be found in the literature [26, 27, 47, 48, 49, 50]

9.3 Interplanetary dust background in the ecliptic plane and above the solar poles

The Ulysses dust measurements provide – as a function of time and spaceprobe position – the flux of particles as a function of impact direction, speed, and particle mass. Here we include data obtained by Ulysses from launch to the completion of the first inclined orbit. Shortly after launch the impact rate of 10^{-17} kg and smaller particles declined from a few impacts per day to about one impact per 3 days (Fig. 9.3). Most of the time of interplanetary cruise until 1996 the dust impact rate stayed at this level. In late 1996 the impact rate decreased again by about a factor of 3. For about one year around Jupiter fly-by the impact rate of the smallest impacts increased by up to a factor of 1000 for periods of one to several days. These dust streams are the second discovery of the Ulysses dust instrument [22]. Their characteristics will be discussed in Section 9.4.

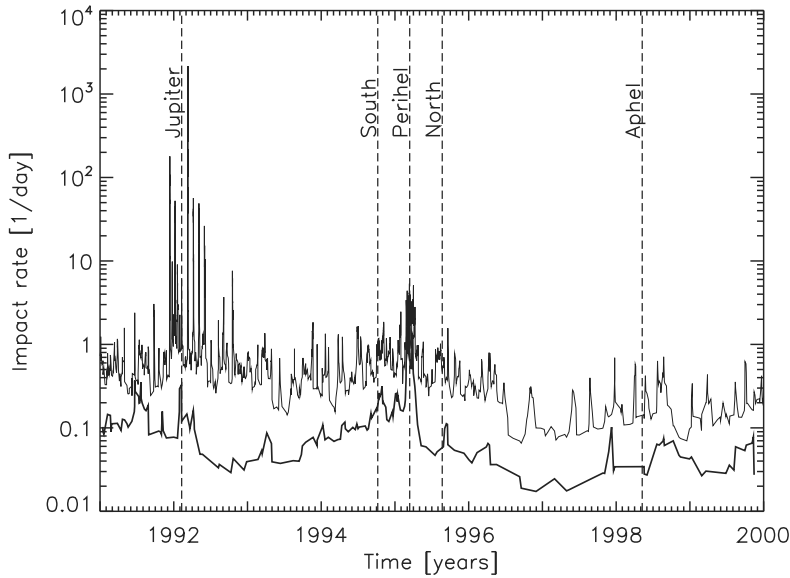


Figure 9.3: Dust impact rates observed by Ulysses. The impact rates shown cover the periods from launch to Jupiter fly-by and the full out-of-ecliptic orbit from Jupiter over the poles of the Sun, through the ecliptic plane (perihelion) and out to aphelion at Jupiter distance. The impact rates are all impacts recorded (upper trace) and impacts of dust particles with $m > 10^{-15}$ kg (lower trace). The impact rates are sliding means always including six impacts.

At high ecliptic latitudes close to the solar poles a surprisingly large dust flux was recorded. Around the time of ecliptic plane crossing the impact rate of big particles ($m > 10^{-15}$ kg) increased by about a factor of 10, whereas less massive particles showed a smaller enhancement. Particles smaller than 10^{-17} kg were recorded in

abundance for some time shortly after launch, around Jupiter fly-by as jovian dust streams, and around the times of the polar passages. These events will be discussed in the sections on β -meteoroids (Section 9.3.2), and on Jupiter dust streams (Section 9.4).

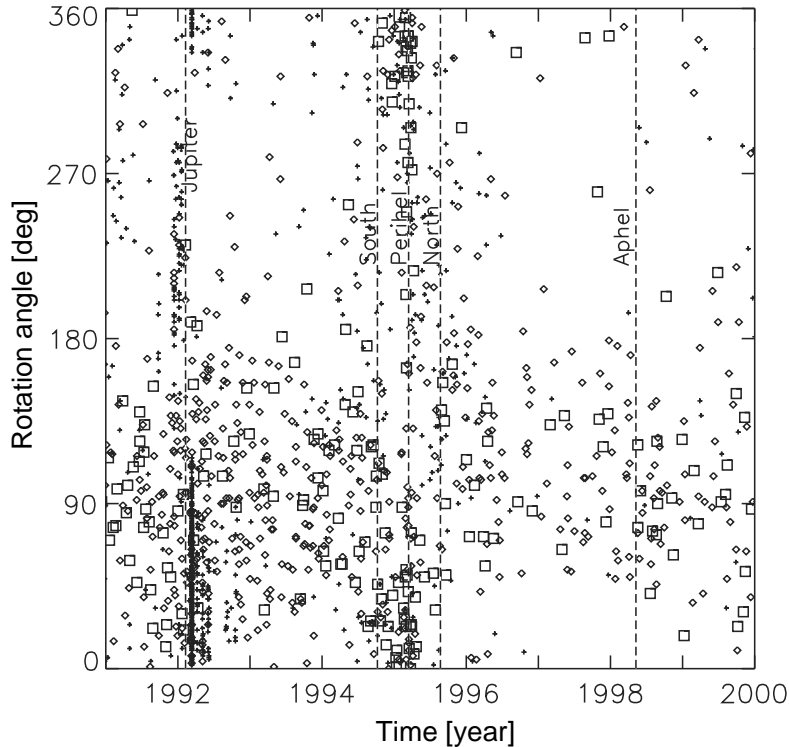


Figure 9.4: Dust impact directions (rotation angle) observed by Ulysses. The rotation angle is defined in Fig. 9.8. The rotation angle is 0° when the dust sensor axis points closest to the ecliptic north pole. At rotation angle 90° the detector axis points parallel to the ecliptic plane in the direction of planetary motion, and at 180° it points closest to the south ecliptic pole. The data cover the periods from launch to Jupiter and a full out-of-ecliptic orbit. The smallest impacts of particles with masses $m \leq 10^{-17}$ kg are denoted by crosses, medium massive particles (10^{-17} kg $< m \leq 10^{-15}$ kg) are denoted by diamonds, and most massive particles ($m > 10^{-15}$ kg) are denoted by squares.

The directional distribution of dust impacts (Fig. 9.4) shows a similar separation in different categories as the impact rate. Here, we concentrate on particles bigger than 10^{-17} kg, smaller particles are discussed in their respective sections. The impact directions were concentrated at rotation angles of about 90° for most of the time. This direction is compatible with the flow direction of interstellar grains through the solar system (cf. Section 9.5). Only around the time of ecliptic plane crossing the mean impact direction shifted to about 0° rotation angle. This direction is compatible with the flux of interplanetary meteoroids around the Sun. Mostly during the passage

from the north pole to Ulysses' aphelion also a few big impacts were recorded from about 270° rotation angle, i.e. the direction one would expect particles on prograde bound orbits to arrive from.

9.3.1 Ulysses' South-North traverse

The Ulysses mission is especially well suited to obtain a latitudinal profile of the interplanetary dust cloud. In the distance range from 2.3 to 1.3 AU, Ulysses passed from close to the ecliptic south pole (-79° ecliptic latitude) through the ecliptic plane to the north pole ($+79^\circ$). The outer portions of the out-of-ecliptic orbit (beyond 2.3 AU) are not suited for characterizing interplanetary dust because of the dominant interstellar dust population [4].

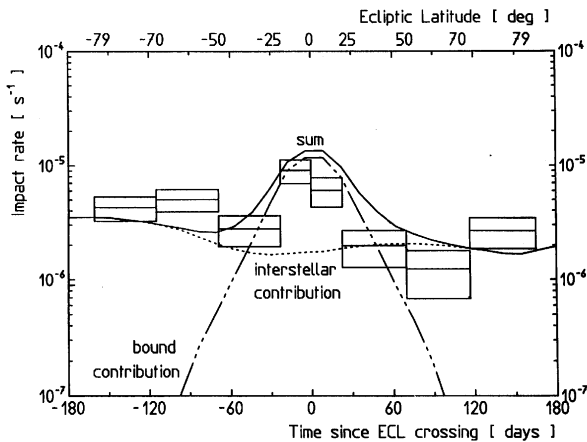


Figure 9.5: Dust impact rate (impact charge $Q_I > 8 \cdot 10^{-14} \text{ C}$) observed by Ulysses during its South-North traverse around the time of ecliptic plane crossing (ECL). The top scale gives the spacecraft latitude. The boxes indicate mean impact rates and standard deviations. The observed impact rates are compared with models of the two major dust components in the solar system: interstellar dust and interplanetary dust on bound orbits about the Sun.

The relation between the dust density at a given latitude and the inclination distribution is simply given by the fact that dust particles recorded at ecliptic latitude λ must have inclinations $i \geq \lambda$ in order to reach this latitude. Figure 9.5 shows the impact rate during the pole-to-pole traverse. The passages over the solar south and north poles occurred 170 days before and after ecliptic plane crossing, respectively. A total of 109 impacts (with impact charges $Q_I > 8 \cdot 10^{-14} \text{ C}$) were recorded during this time. The impact rate stayed relatively constant except for the maximum ($9 \cdot 10^{-6} \text{ s}^{-1}$) during ecliptic plane crossing. The impact rate at the northern leg is about a factor of 2 below that of the southern one. This is due to the varying spacecraft attitude which followed the direction to the Earth. This variation of spacecraft attitude is also reflected in the variations of rotation angles of the impacts which

were detected during the S-N traverse. Over the south solar pole most large impacts (with impact charges $Q_I > 8 \cdot 10^{-14}$ C) occurred at rotation angles between 0° and 150° which includes the interstellar direction (cf. Fig. 9.7). Closer to the ecliptic plane the rotation angle range of large impacts widened and moved further to the north direction (rotation angle $\sim 0^\circ$). At ecliptic plane passage these impacts were recorded in a wide range around the north direction (0° to 100° and 200° to 360°). On the northern pass, rotation angles covered the whole range and above the north pole it ranged from 50° to 200° , again including the interstellar direction.

Figure 9.6 shows the masses of dust particles detected during the S-N traverse. 20 particles with masses greater than 10^{-13} kg were detected during the S-N traverse, 15 of these particles were recorded during the 80 days when the spacecraft was close to the ecliptic plane ($-30^\circ < \lambda < 30^\circ$). This increased flux of big particles near the ecliptic plane is obviously due to the zodiacal dust population. The mass distribution during the S-N traverse seems to be composed of two distinct components: the interstellar dust component, which has peak masses between 10^{-14} and 10^{-15} kg and a bigger interplanetary dust component dominating the dust flux in the near-ecliptic region.

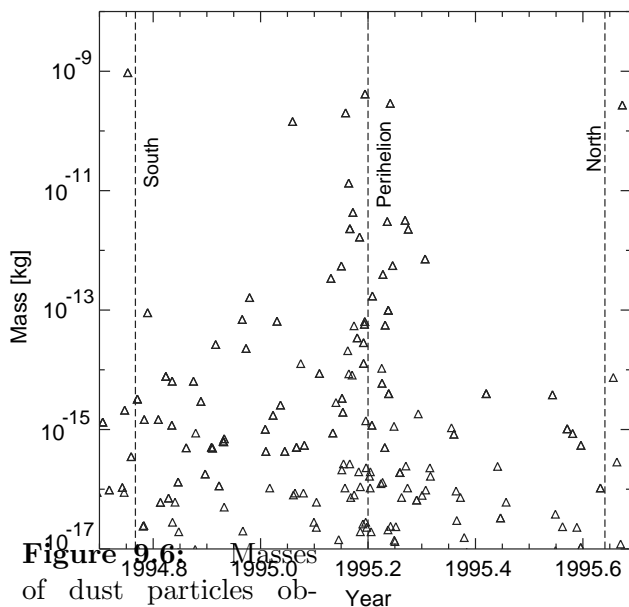


Figure 9.6: Masses of dust particles observed by Ulysses during its South-North traverse. Ecliptic plane crossing coincided with perihelion passage.

9.3.2 β -meteoroids

β -meteoroids are particles that leave the solar system on hyperbolic orbits because of radiation pressure and electromagnetic solar wind interactions [34]. They could only be observed by Ulysses for a few short periods during the Ulysses mission: the early mission phase, both polar passes [4], and the perihelion ecliptic plane crossing. Wehry and Mann [71] have identified β -meteoroids in the Ulysses data set and discuss some properties.

9.3.3 Mass distribution of interplanetary particles

Although Galileo and Ulysses dust data cover a mass range $10^{-19} \text{ kg} \leq m \leq 10^{-9} \text{ kg}$, the statistically best and most complete measurements range only from $10^{-17} \text{ kg} \leq m \leq 10^{-12} \text{ kg}$. The mass distribution of the interplanetary dust is best known near the Earth. It has been determined from lunar crater counts and Earth-orbiting spacecraft (Pegasus, Explorer 16 and Explorer 23, Pioneer 8 and Pioneer 9, LDEF and many others). Here we will use the mass distribution which Divine [12] derived from the measurements presented by Grün et al. [19]. In addition we will use the radial dependence of the dust density that is based on zodiacal light observations by Helios [56].

9.3.4 Description of model distributions

Several dynamical meteoroid models have been developed in the last decades to describe the interplanetary meteoroid environment. The most comprehensive one so far is the model of Divine [12] and its extension by Staubach [69, 70] that synthesizes meteor data, zodiacal light observations, and in-situ measurements of interplanetary dust. The model describes dust concentrations and fluxes on the basis of meteoroid populations with distinct orbital characteristics. Gravitational (keplerian) dynamics and radiation pressure effects are employed in order to derive impact rates. Besides impact rates, impact directions and speeds can be modeled. The model includes dust populations on bound orbits around the Sun and an interstellar dust population that penetrates the solar system on unbound trajectories.

For the model description of interplanetary micrometeoroids we follow in principle the method of Divine [12] with the extension introduced by Staubach [69, 70]. The spatial dust density and the directional dust flux at each position in interplanetary space are synthesized from 'model' distributions of orbital elements. Following Divine [12] the interplanetary meteoroid complex is represented by several populations of dust particles that are defined by their orbital elements and mass distributions. In order to simplify the meteoroid model, several assumptions have been made: (1) the zodiacal dust cloud is symmetric about the ecliptic plane, and (2) it has rotational symmetry about the ecliptic polar axis. Therefore, in the model the spatial dust density depends only on distance r from the Sun and height z above the ecliptic plane. Small asymmetries relative to the ecliptic plane [55] or a small offset of the

cloud center from the Sun [11] are ignored. No time dependences are considered, although for the sub-micrometer dust flux a 22-year cycle has been suggested from theoretical considerations [62, 32, 34] and found in the data [51, 53, 54].

In addition to solar gravity, orbits of micrometer-sized dust grains are affected by solar radiation pressure. The ratio of radiation pressure force, F_{rad} , to gravitational attraction by the Sun, F_{grav} , is defined by the factor $\beta = F_{\text{rad}}/F_{\text{grav}}$ [9]. This β -value is strongly dependent on material composition and structure of the dust particles. In the dynamical dust model, β -values obtained by Gustafson (1994) from Mie calculations for homogeneous spheres are assumed. For particles with masses $m > 10^{-13}$ kg the influence of radiation pressure is negligible. At 10^{-14} kg, 10^{-16} kg, and $5 \cdot 10^{-18}$ kg β -values of 0.3, 0.8, and 0.3, respectively, have been assumed. These values represent a continuous dependence and reflect the combination of the solar spectrum and particles size. For bound orbits $\beta < 1$ is required.

In order to evaluate the flux at position \mathbf{r} (bold characters indicate vector quantities) the dust particle velocity, \mathbf{v} , has to be determined from the orbital elements, perihelion distance, r_1 , eccentricity, e , and inclination, i , and from the assumed β -value. The relative velocity \mathbf{u}_D between a dust particle and the spacecraft with velocity \mathbf{v}_{DB} is then $\mathbf{u}_D = \mathbf{v} - \mathbf{v}_{DB}$. The sensitivity of a detector can be expressed by its mass threshold m_t and its angular sensitivity. For spinning spacecraft like Galileo and Ulysses the effective sensitive area, Γ , is a function of the angle, γ , between the impact direction and the spacecraft axis [20].

Populations of interplanetary meteoroids are described by independent distributions of orbital inclination $p_i(i)$, eccentricity $p_e(e)$, perihelion distance $N_1(r_1)$, and particles mass $H_M(m)$, and the corresponding β -values. The detector threshold m_t , and the angular sensitivity Γ are used as weighting factors for the calculated flux [12] [29]. For any assumed dust population (defined by its distribution functions) and a given observation condition (spacecraft position, \mathbf{r}_{DB} , velocity, \mathbf{v}_{DB} , detector orientation, \mathbf{r}_D , and sensitivity weighting factors), model fluxes and spatial densities can be calculated.

The distribution functions have been iterated by comparison with the corresponding measurement: the difference between the measurement and the sum of model fluxes of all dust populations is expressed by a residual. Each distribution function consists of a limited number of parameters (e.g. the inclination and eccentricity distributions are represented by seven parameters each) which were varied by an iteration algorithm in such a way that the residual was minimized.

Populations of particles on heliocentric bound orbits have been defined by the procedure described above. The populations are ad hoc populations used for fitting purposes and do not correspond to specific sources of dust. Divine's core population (and the corresponding orbital distribution) has been found to fit micrometeoroids of masses $m > 10^{-13}$ kg that are not affected by radiation pressure. Three populations of smaller meteoroids, with $\beta > 0$, on bound heliocentric orbits fit the smaller particles detected by Galileo and Ulysses, mostly inside 3 AU distance from the Sun. Although all populations are defined over the whole mass range (10^{-21} kg $\leq m \leq 10^{-3}$ kg) each

population dominates in a narrow mass interval for which a constant β -value has been assumed. The interstellar dust population is well represented by Ulysses and Galileo dust measurements at large heliocentric distances [22, 24, 5]. The interstellar dust flow is, within the measurement uncertainties, aligned with the flow of interstellar gas through the heliosphere [72]. Observed dust speeds are compatible with the 26 km s^{-1} unperturbed gas speed. About 60% of the interstellar grains have masses between 10^{-17} kg and 10^{-15} kg . With an assumed value of $\beta = 1$, interstellar grains pass on straight trajectories through the planetary system. This β value is typical for the bulk of interstellar grains observed by Ulysses (for a detailed discussion see [52]). Model fluxes are calculated with these assumptions.

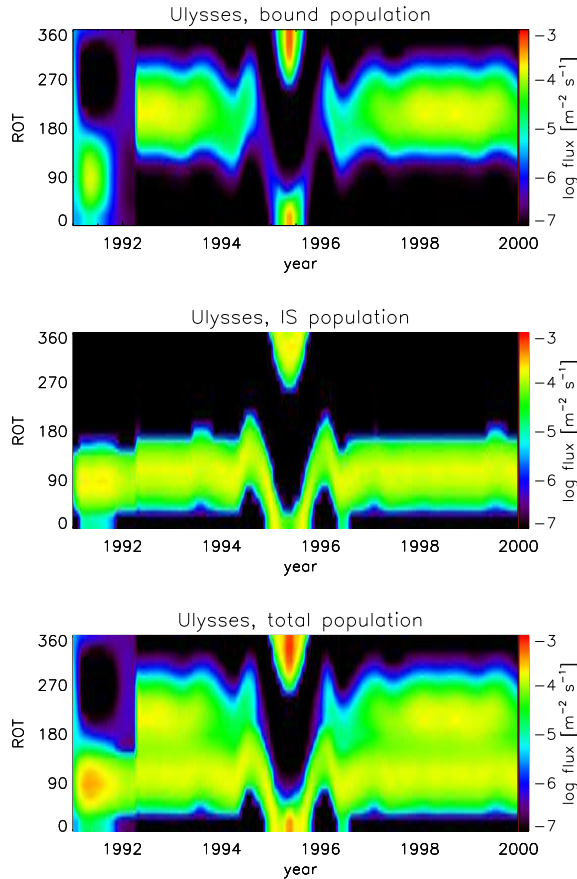


Figure 9.7: Models of directional impact rates (of particles with masses $m > 10^{-17} \text{ kg}$) onto Ulysses from launch to completion of its first out-of-ecliptic orbit. The color coding of flux values is shown on the right side of each panel. Impact rates of interplanetary dust on bound orbits (upper panel), interstellar dust (middle panel), and the total impact rate (lower panel) are shown. The total impact rate can be compared with the observed directional impact rates in Fig. 9.4 (the number of impacts – diamonds and squares – in a time and a rotation angle interval corresponds to the modelled impact rate).

Fig. 9.7 shows the calculated directional fluxes for the considered time period. The flux values are color coded and represent the flux in a phase space interval, ΔROT and Δt . These model fluxes can be compared with the measurements shown in Fig. 9.4 where the number of impacts in the same phase space interval should be

considered.

9.3.5 Comparison with zodiacal light

The model can be used to derive the global interplanetary dust distribution as represented by visible zodiacal light and infrared thermal emission observations. The latitudinal density distribution was derived from zodiacal light observations [56] or from infrared observations with COBE [65]. Infrared brightnesses like those observed by COBE observations were taken in a band approximately perpendicular to the solar direction and, therefore, refer to dust outside Earth's orbit and do not represent dust close to the Sun (this is in contrast to zodiacal light observations which can be performed in almost any direction). The difference between the density distributions that fit the observed zodiacal and infrared brightnesses suggests that zodiacal dust in the inner solar system has a wider distribution (to which the zodiacal light measurements refer) than dust outside the Earth's orbit to which COBE data refer. Divine's core population approximates the latitudinal density function of zodiacal light observations for low latitudes ($\lambda < 10^\circ$) and that of infrared observations for high latitudes ($\lambda > 20^\circ$). The density distributions for the small particle populations have a wider latitudinal distribution and are closer to the zodiacal light distribution. The assumed constant density of interstellar dust provides a small but constant contribution at all latitudes.

From the dust populations, Grün et al. [29] have calculated model brightnesses of the zodiacal light as observed from Earth. By far the largest contribution comes from the core population with masses $m > 10^{-13}$ kg. Particle populations with masses $m < 10^{-13}$ kg contribute less than 1% to the zodiacal light brightness at 1 AU. In order to obtain this result it was assumed that the albedo (ratio of visual light reflected by a grain to the amount of incident light) is $p = 0.05$ for the core population and $p = 0.02$ for the asteroidal population. We had to assume that the small particle populations consist of very dark particles (albedo of $p = 0.01$) in order for the sum of all populations not to exceed the observed brightness.

9.4 Electromagnetically interacting dust: Jupiter Dust Streams

9.4.1 Observations

On 10 March 1992, about one month after Jupiter fly-by, perhaps one of the most unexpected findings of the Ulysses mission has been detected: an intense stream of dust grains which was soon recognized to originate in the Jupiter system [3]. During this burst more than 350 impacts were detected within 26 hours. This exceeded by more than two orders of magnitude the typical impact rates of interplanetary and interstellar dust seen before. Ten more such dust streams could be revealed in the

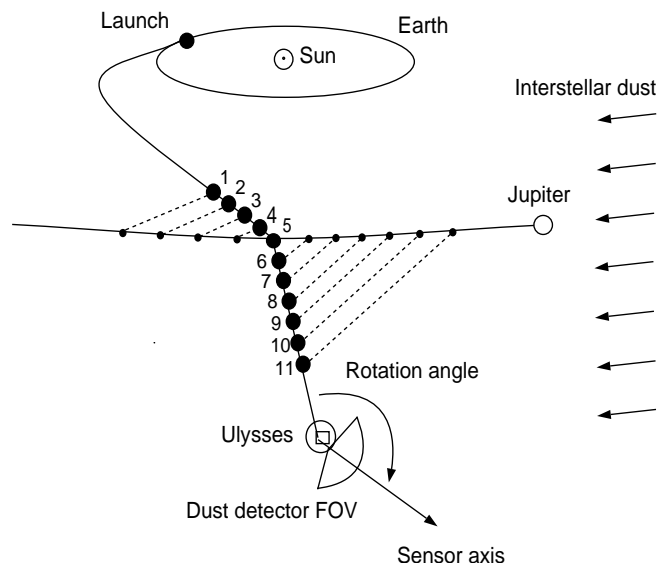


Figure 9.8: Ulysses trajectory and geometry of dust detection – oblique view from above the ecliptic plane. The position of the Sun and orbits of Earth and Jupiter (in the foreground) are also shown. The trajectory of Ulysses after Jupiter closest approach is deflected into an orbit inclined by 79° to the ecliptic plane going south. Numbers along the trajectory refer to positions of Ulysses at which dust streams were detected, dotted lines point to Jupiter. The spacecraft spins about an axis which points towards Earth. The dust detector on board has a 140° conical field of view (FOV), and is mounted almost at a right angle (85°) to the Ulysses spin-axis. Radiant directions from which it can sense impacts therefore include the plane perpendicular to the spacecraft-Earth line. The rotation angle of the sensor axis at the time of a dust impact is measured from the ecliptic north direction. Arrows indicate the approach direction of interstellar dust.

data when Ulysses was within 2 AU from Jupiter [22, 3]. The geometry of dust detection during Ulysses' Jupiter fly-by is shown in Fig. 9.8 and the observed impact rate which shows the dust streams as individual spikes is displayed in Fig. 9.9. The streams occurred at approximately monthly intervals (28 ± 3 days). No periodic dust phenomenon in interplanetary space was known before for small dust grains. Details of the streams are summarised in Tab. 9.1.

The impact direction (rotation angle) of the dust stream particles is shown in Fig. 9.10. The Jupiter system was the most likely source of the streams because of the following reasons: 1) the streams were narrow and collimated, which required a relatively close-by source. Otherwise they should have been dispersed in space and time; 2) the streams were concentrated near Jupiter and the strongest one was detected closest to the planet; 3) the streams before Jupiter fly-by approached Ulysses from directions

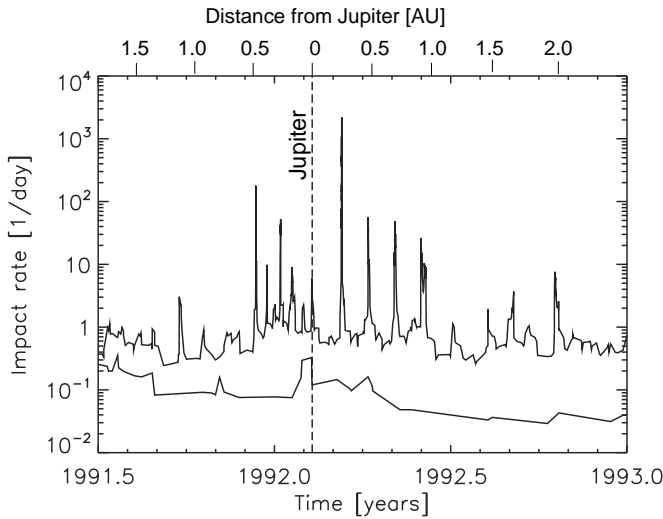


Figure 9.9: Impact rate of dust particles observed by Ulysses around Jupiter fly-by. The curves show all impacts recorded (upper curve) and impacts of dust particles with masses greater than 10^{-15} kg. The impact rates are means always including six impacts. The distance from Jupiter is indicated at the top.

almost opposite to the streams from after fly-by. All streams, however, radiated from close to the line-of-sight direction to Jupiter. 4) The observed periodicity suggested that all streams originated from a single source and seemed to rule out cometary or asteroidal origins of individual streams. Especially, comet Shoemaker-Levy 9, before its tidal disruption in 1992, was considered as a possible source [23]. Only two of the eleven streams, however, were compatible with an origin from the comet.

Confirmation of the Jupiter dust streams came from Galileo: dust “storms” with up to 10,000 impacts per day were recorded about half a year before Galileo’s arrival at Jupiter when the spacecraft was within 0.5 AU from the planet [28]. Later, with Galileo, the dust stream particles were detected within Jupiter’s magnetosphere [30, 31]. The data showed a strong fluctuation with Jupiter’s 10 hour rotation period which demonstrated the electromagnetic interaction of the dust grains with the ambient magnetic field of Jupiter. The dust streams seen in interplanetary space are the continuation of the streams detected by Galileo within the magnetosphere.

9.4.2 Particle Masses and Speeds

The dust instruments on board Ulysses and Galileo have been calibrated in the laboratory. The calibrated range covers 3 to 70 km s^{-1} in speed and 10^{-9} to 10^{-19} kg in mass [25]. By applying these calibrations, masses and speeds of the stream particles were $1 \cdot 10^{-19}$ kg to $9 \cdot 10^{-17}$ kg and 20 to 56 km s^{-1} , respectively. Uncertainties for

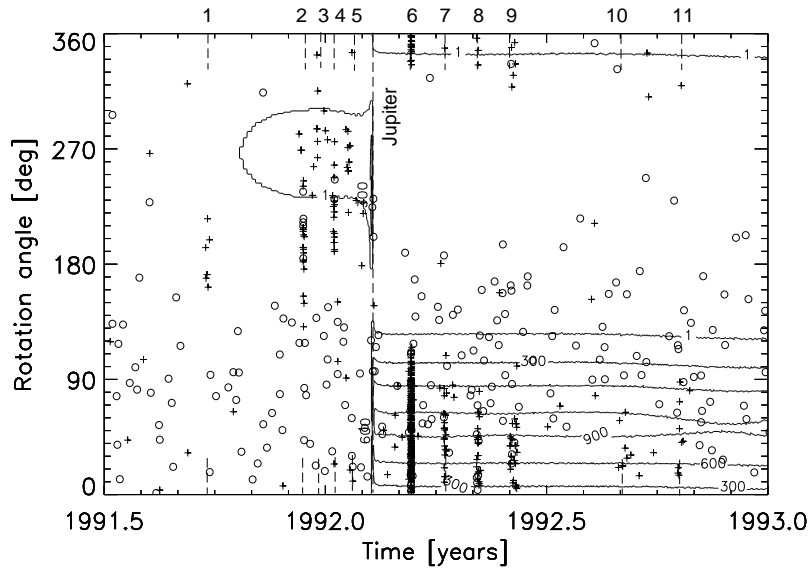


Figure 9.10: Dust impact directions observed around Jupiter fly-by. Crosses denote particles with masses $m < 10^{-17}$ kg, circles denote particles with $m > 10^{-17}$ kg. The dust streams are indicated by dashed lines and are labelled 1 to 11. Closest approach to Jupiter is indicated by a long dashed line. The contours show the sensitive area of the dust sensor for particles approaching on straight lines from the line-of-sight to Jupiter.

the velocity were a factor of 2, and, for the mass, a factor of 10. Assuming an average density of 1 g cm^{-3} the derived sizes of the particles were 0.03 to $0.3 \mu\text{m}$. These values, however, were challenged by later investigations:

Although the particles' approach directions were close to the line-of-sight to Jupiter, the approach direction of most streams deviated too much from the direction to Jupiter to be explained by gravitational forces alone. The deviation of the stream direction from the Jupiter direction was correlated with the magnitude and direction of the interplanetary magnetic field (especially its tangential component). Strong non-gravitational forces must have been acting on the grains to explain the observed impact directions. In numerical simulations Zook et al. [74] integrated the trajectories of many particles backward in time and away from Ulysses in various directions (Fig. 9.11). Only particles which came close to Jupiter (< 100 Jupiter radii) were considered compatible with a jovian origin. The dust particles were assumed to be electrically charged to $+5 \text{ V}$ by a balance between solar photo-electron emission and neutralization by solar wind electrons. The solar wind speed was assumed to be 400 km s^{-1} . Forces acting on the particles included Sun's and Jupiter's gravity and the interaction with the interplanetary magnetic field as observed by Ulysses [7].

One important result from this analysis was that the particles were about 10^3 times less massive and 5 to 10 times faster than the values implied by the calibration of the dust instrument. Only particles with velocities in excess of 200 km s^{-1} and masses of the order of 10^{-21} kg were compatible with an origin in the Jupiter system. The

Table 9.1: Parameters of the Jupiter dust streams adopted from Baguhl et al. [3]. The time corresponds to the center of the burst. Closest approach to Jupiter occurred on 92-039.5. Jupiter radius is $R_J = 71,492$ km.

Stream number	Days from Jupiter fly-by	Date (yr-day) Duration (h)	Number of particles	Mean rotation angle (deg)	Distance to Sun (AU)	Distance to Jupiter(R_J)
Stream 1	-136.7	91-267 76.0	6	182	4.30	2356
Stream 2	-57.8	91-346 10.4	21	193	4.93	996
Stream 3	-45.8	91-358 18.0	7	295	5.08	796
Stream 4	-32.1	92-007 10.5	15	224	5.14	561
Stream 5	-20.4	92-019 57.1	10	259	5.29	367
Stream 6	31.2	92-071 34.3	327	49	5.4	549
Stream 7	59.4	92-099 60.9	28	47	5.39	1017
Stream 8	87.4	92-126 55.6	33	29	5.38	1484
Stream 9	116.7	92-156 107	28	25	5.36	1965
Stream 10	205.4	92-244 215	12	29	5.32	3418
Stream 11	254.3	92-293 103.4	13	57	5.2	4200

corresponding particle radii were only 5 to 10 nm. Particles smaller than 5 nm were unable to travel from Jupiter to Ulysses. They were rather caught up by the solar wind and swept away. Particles significantly larger than 25 nm were not compatible with the measured impact directions because they did not interact strongly enough with the interplanetary magnetic field. For 10 nm sized particles the Lorentz force exceeds gravity by more than a factor of 1,000 and the trajectories of such particles are totally dominated by the interaction with the interplanetary magnetic field. Although the simulated impact directions can explain the observations, Ulysses should have detected particles in between the dust streams when no impacts were detected. This indicates that apart from interaction with the interplanetary magnetic field there must be other processes that modulate the particle trajectories.

The analysis by Zook et al. has demonstrated that the solar wind magnetic field acts as a giant mass-velocity spectrometer for charged dust grains. In particular, masses and impact speeds of the grains derived from the instrument calibration [25] were shown to be invalid for the tiny Jupiter dust stream particles. Masses and speeds of stream particles derived from the Galileo measurements agreed very well with the values obtained for the streams detected by Ulysses (J.C. Liou and H. Zook, priv. comm.).

9.4.3 Dust Source and Particle Acceleration in Jupiter's Magnetosphere

What is the source of the dust streams in the Jupiter system, and which mechanism can accelerate the grains to sufficiently high speeds so that they are ejected into inter-

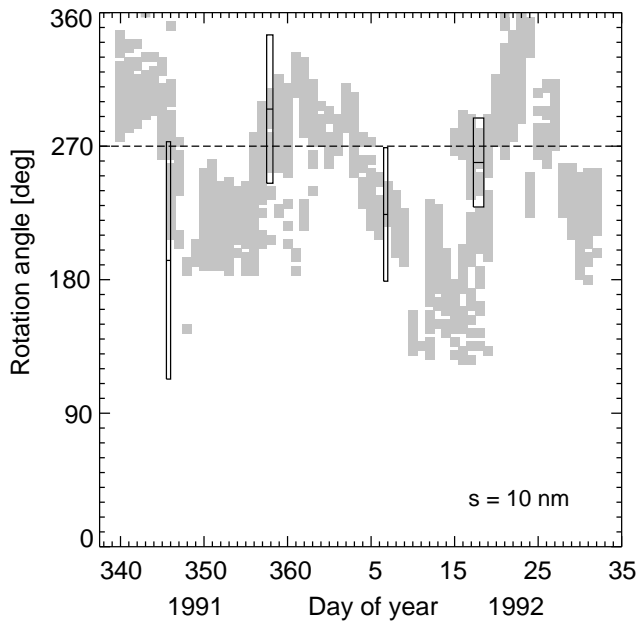


Figure 9.11: Simulated arrival directions (rotation angle) of 10 nm dust particles from Jupiter to Ulysses (shaded area) compared with directions from which dust streams were observed by the Ulysses dust sensor (boxes; from Zook, priv. comm.) The box sizes indicate the duration and range of impact directions.

planetary and, possibly, interstellar space? One possible source was suggested even before the arrival of the two Voyager spacecraft at Jupiter in 1979: the volcanoes on Io [45, 64]. Small grains entrained in volcanic plumes follow ballistic trajectories and reach altitudes where they become exposed to the Io plasma torus. When grains encounter this high-density plasma region, they rapidly collect electrostatic charge and interact with the local magnetic field. For grains smaller than $0.1 \mu\text{m}$, the resulting Lorentz force overcomes Io's gravity and these grains become injected into Jupiter's magnetosphere. The injection velocity is the relative velocity between the co-rotating magnetic field and Io, i. e., 57 km s^{-1} . This production mechanism sets an upper limit on the size of the dust particles escaping from Io.

Dust grains which are positively charged and released at Io's distance ($r = 5.9 R_J$, Jupiter radius $R_J = 71,492 \text{ km}$) are accelerated outward and leave the Jupiter system if their radii are between about 9 nm to 180 nm [31]. Smaller particles remain tied to the magnetic field lines and gyrate around them like ions do. Bigger grains move on gravitationally bound orbits which are affected by the Lorentz force. The size range of expelled particles narrows down if the source is located closer to Jupiter, with the upper size limit staying approximately constant at 180 nm. For example, at the outer distance of the gossamer ring ($3R_J$) the lower size limit is 28 nm [33]. This radial

variation of the lower size limit of expelled particles is an indication of the source distance from Jupiter [31]. Sizes of ejected grains of about 10 nm as determined by Zook et al. [74] are compatible with an Io source but contradict a source significantly closer to Jupiter, like e.g. the gossamer ring.

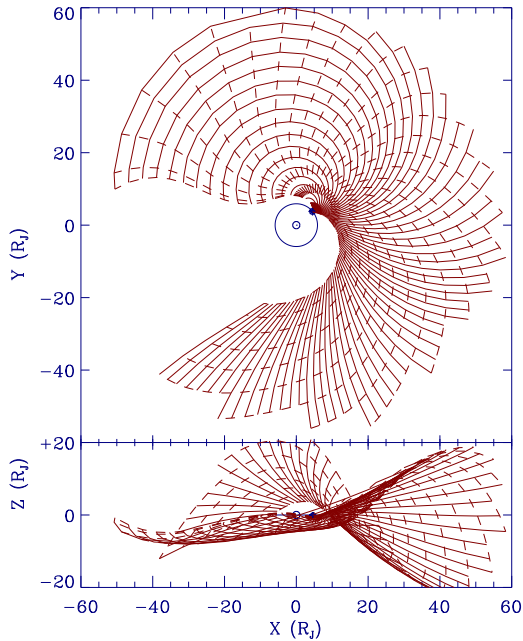


Figure 9.12: Jupiter’s ‘dusty ballerina skirt’ formed by Jupiter stream particles moving away from the planet in a warped dust sheet [31]. Jupiter is in the center and the particles are released from a point source at Io’s distance. The dust sheet is defined by synchrones (solid lines, positions of dust particles released at the same time) and syndynes (dashed lines, positions of dust particles which have the same charge-to-mass ratio, q/m). Adjacent synchrones are 1332 sec apart. Syndynes of differently sized particles range from $s = 9.0$ nm to $s = 100$ nm, or, alternatively, at a surface potential of $U_g = +3$ V to q/m -values between 984 and 8 C kg^{-1} . Particle trajectories have been followed only out to $50 R_J$ which causes the ragged outer edge of the dust sheet. In steady state the dust sheet extends to much larger distances. The configuration of the dust sheet depends strongly on the phase of the magnetic field.

To a first order approximation, particles which are released from a source close to Jupiter’s equatorial plane (e.g. Io or the gossamer ring) are accelerated along this plane. Beside this outward acceleration, however, there is a significant out-of-plane component of the electromagnetically induced force because Jupiter’s magnetic field is tilted by 9.6° w.r.t. to the planet’s rotation axis. Thus, the dust particles are deflected out of Jupiter’s equatorial plane where they originated: Particles which are continuously released from a point source move away from Jupiter in a warped dust sheet, where particles are separated according to their size (or more appropriately

to their charge to mass ratio) and time of generation. This scenario is depicted in Fig. 9.12. A detector in Jupiter’s equatorial plane detects an increased number of particles when this dust sheet passes over its position. Fluctuations in the dust impact rate with 5 and 10 h periods and impact directions observed by Galileo [30, 31] can be explained by grains which are electromagnetically coupled to the magnetic field. However, only particles with a narrow size range of about 10 nm can explain the observed features. Modelling implies that larger or smaller particles have not been detected by the Galileo dust instrument. The 28 day periodicity detected by Ulysses in interplanetary space (cf. Fig 9.9) can be explained by a resonance between the rotation period of Jupiter (and, hence, its magnetic field) and Io’s orbital period [40]. Although modelling results are compatible with Io being the source of the dust stream particles, modelling alone could not prove the source. In addition to the 5h and 10h periods which are compatible with Jupiter’s rotation period, a modulation of the impact rate with Io’s orbital period (42 h) was found in the data [46]. A periodogram which transformed two years of impact rate data into frequency space shows an amplitude modulation of Jupiter’s magnetic field frequency and Io’s orbital frequency (Fig. 9.13; [16]). The periods of the magnetic field and Io modulate each other, and the only explanation is Io being the source of the “carrier frequency”. Photometric observations of the Io plumes obtained with Voyager imply a size range of 5 to 15 nm [10] and recent Hubble Space Telescope observations constrained the particles to be smaller than 80 nm [68]. This is compatible with the results of Zook et al. [74].

The characteristic signature of an amplitude modulation of oscillation frequencies is a carrier frequency (ω_0) with side frequencies, or “modulation products,” ($\omega_1 + \omega_0$) and ($\omega_1 - \omega_0$). If Io’s orbital frequency is a carrier frequency, and charged dust trapped in Jupiter’s magnetic field is a frequency of Jupiter’s rotation, that is amplitude-modulating Io’s signal, then one would see a frequency at Jupiter’s rotation period with side frequencies plus and minus Io’s orbital frequency. The frequency-transformed data obtained with Galileo directly display this amplitude-modulation scenario.

The dynamics of the charged nanometer-sized dust particles which are released from Io, pass the Io torus and are finally ejected out of Jupiter’s magnetosphere is strongly affected by the geometry of the magnetic field. In a completely radially symmetric magnetic field configuration no 10 h period should be evident in the impact rate, only the 5 h period should be seen. The prominent modulation of the rate with the 10 h period indicates that there must be a variation in the acceleration of the particles which is correlated with jovian local time. The Io dust stream particles will serve as test particles for future investigations of the jovian magnetic field environment.

9.5 Interstellar Dust

Prior to the Ulysses dust measurements, the abundance and even the mere existence of interstellar dust grains inside the solar system was controversial. Interstellar grains

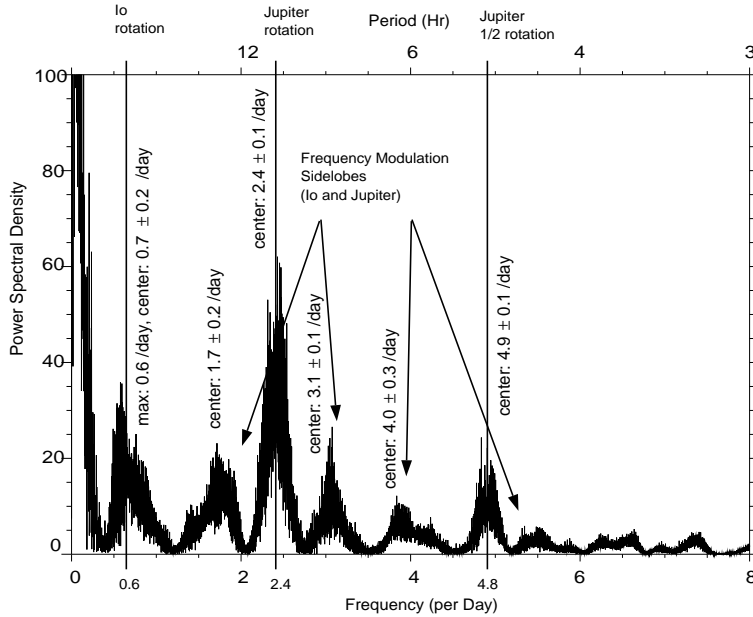


Figure 9.13: A Scargle-Lomb periodogram [66] for two years of Galileo dust data (1996 and 1997; from [16]). A source with a 10 h period, Jupiter’s magnetic field, is modulated by Io’s frequency which leads to peaks at 13.9 and 7.7 h. There are additional frequencies, a half period of Jupiter’s magnetic field (4.9 h), Io as a single source (41.9 h), and a low-frequency oscillation trend due to the spacecraft orbital geometry.

which are not bound to the Sun or any other star, but belong to the interstellar medium of our Galaxy, should pass by the Sun on its way through that medium. By using the density of the interstellar medium surrounding the solar system and the general assumption that 1% of the mass of the interstellar medium is contained in dust grains [39], it was postulated that the flux of these grains in the solar system has to be of the order of $10^{-3} \text{ m}^{-2} \text{ s}^{-1}$. This is higher than the total flux of cosmic dust observed at Earth orbit [19]. This non-detection lead to the conclusion that there has to be a physical process which removes interstellar dust from at least the inner solar system. Levy and Jokipii [60] showed that the dominant force on small dust grains in the solar system is the Lorentz force caused by the solar wind magnetic field sweeping by the electrically charged dust grains. Electron emission due to solar UV photoeffect, in equilibrium with the sticking of electrons from the surrounding plasma environment, charges the grains to a positive surface potential. Since the Lorentz force acts perpendicular to the solar wind velocity vector, this seemed to be a mechanism for diverting the stream of interstellar dust grains out of the solar system. Nonetheless, it was argued [32, 63] that the Lorentz force not only diverts, but also concentrates interstellar dust, depending on the phase of the solar cycle. Furthermore, the Lorentz force is not as effective on larger grains as it is on small

ones, because it accelerates grains proportional to their charge-to-mass ratio q/m . The charge-to-mass ratio, in turn, is inversely proportional to the grain radius s , if a constant surface potential and a spherical shape of the grain are assumed.

The size range $0.005 \mu\text{m} \leq s \leq 0.25 \mu\text{m}$ of classical interstellar dust grains, which have been postulated to explain the extinction of starlight [61], indicated that these grains should be heavily affected by interaction with the solar wind magnetic field. Before Ulysses the proposed properties of interstellar dust were

- (a) there are no big ($s > 0.25 \mu\text{m}$) dust grains in the diffuse interstellar medium surrounding the Sun, and
- (b) the small ones are prevented from entering the planetary system by the solar wind magnetic field.

9.5.1 Discovery and Identification of Interstellar Dust Grains

After Ulysses had flown by Jupiter in February 1992, dust impacts were detected predominantly from a rotation angle between 0° and 180° . As can be seen in Figure 9.8, this corresponds to grains approaching from the retrograde direction. Significantly fewer impacts were detected from the prograde direction from which grains released from solar system bodies are expected, (cf Figure 9.4). Attempts to explain the measurements by a population of retrograde interplanetary grains failed because the impact rate of grains from the retrograde direction was constant while Ulysses was moving to higher and higher heliocentric latitudes [6]. Since the impact rotation angle of about 100° coincided with the upstream direction of gas from the local interstellar medium [72], it was concluded that Ulysses detected particles belonging to a stream of dust grains originating from the interstellar medium [22]. In this respect the delay of the Ulysses mission and the resulting change in the final orbit turned out to be fortunate. On the initially planned orbit the Ulysses spin-axis would have pointed nearly parallel to the upstream direction of the interstellar dust most of the time. Since the dust detector points nearly perpendicular to the spin-axis, the impact rate of interstellar dust grains would have been strongly reduced and the identification of interstellar impacts would have been much more difficult.

To support the evidence for interstellar grains in the solar system, the impact velocities of grains detected from the retrograde direction after Jupiter fly-by have been analyzed. Most measured impact velocities, although uncertain by up to a factor of 2, indicated that the grains had heliocentric velocities in excess of the local solar system escape velocity, even if radiation pressure effects were neglected [24]. Analysis of the data collected with the Galileo dust instrument further supported the interpretation of the Ulysses data as impacts of interstellar grains [5]. The discovery of interstellar grains in the solar system contradicted the considerations of the removal of interstellar dust summarized in points (a) and (b) above. This contradiction is resolved by the following considerations

- (A) interstellar grains with radii larger than $0.25 \mu\text{m}$ exist in the diffuse medium. They cannot be detected by measuring the extinction of starlight because they scatter and absorb light independently of the wavelength of the incident radiation. Therefore they do not influence the shape of the interstellar extinction curve, and
- (B) the solar wind magnetic field can indeed concentrate interstellar grains in the solar system. This depends on the phase of the solar cycle [32].

After it was settled that the data set gathered by the Ulysses dust detector contains interstellar grains and that they dominate the impacts detected in the outer solar system, the question was raised how we can distinguish them from impacts of interplanetary grains. In other words, how can we find a subset of the Ulysses dust data which contains only impacts from interstellar grains with high confidence?

As described above, the impact direction is the major characteristic that distinguishes interstellar from interplanetary grains in the outer solar system. Therefore, the identification criterion for interstellar impacts in the Ulysses data set is:

Impacts that have been detected (a) after Ulysses left the ecliptic plane, and (b) with a rotation angle for which the interstellar gas upstream direction lies within the field of view of the dust detector (plus a 10° margin) are preliminarily identified as interstellar impacts.

The so defined data set still contained a contribution from interplanetary impacts because during the short time of the first perihelion passage of Ulysses around March 1995, interplanetary grains hit the detector from the same direction as interstellar grains. Furthermore, Hamilton et al. [34] suggested that very small ($s < 0.1 \mu\text{m}$) interplanetary grains can reach high latitudes when they are electromagnetically ejected from the solar system during favorable phases of the solar cycle. These grains can also contribute to the data set defined above. Therefore, impacts have been removed from the preliminary data set that a) have been measured around ecliptic plane crossing ($\pm 60^\circ$ ecliptic latitude), or b) that have been measured above the solar poles with very small impact signals ($Q_I < 10^{-13} \text{ C}$), indicating small masses.

In Fig. 9.4 we show all dust impacts detected by Ulysses in a rotation-angle-vs-time diagram. The majority of particles in the intermediate mass range is compatible with an interstellar origin. They dominate in the outer solar system.

9.5.2 Mass Distribution and Cosmic Abundances

As explained above, the existence of interstellar grains in the solar system can be explained by the fact that they are too big to be swept away by the solar wind magnetic field. Why can the dust models based on extinction measurements not simply be extended to account for big grains? The reason is that the mass of solid matter in the interstellar medium is limited by the *cosmic abundance of heavy elements*. The most abundant elements in the Galaxy are hydrogen and helium. In dust grains the

amount of both of these elements is negligible as compared to heavier elements. The mass contained in solid dust grains is therefore limited by the available mass contained in elements heavier than helium. On average, 99% of the mass of the local interstellar medium is carried by hydrogen and helium atoms [39]. Therefore, the total mass of dust grains cannot exceed 1% of the overall mass of the medium.

If we calculate a mass distribution of the dust grains, the contribution of each grain mass interval to the total dust mass can be determined. The mass distribution for previous interstellar grain models postulates that most mass is contained in the large grains, although they are less abundant. If this grain mass distribution were extrapolated to infinitely high masses, the total mass contained in dust grains would be infinite. This would contradict cosmic abundance measurements. Therefore, the big interstellar grains found by Ulysses are important for understanding the composition of the interstellar medium.

We can quantify the contribution of the grains measured by Ulysses to the overall mass in dust in the interstellar medium by calculating the mass distribution for the Ulysses measurements and comparing it with the mass distribution of existing interstellar dust models. The mass distribution of interstellar grains measured by Ulysses is shown in Figure 9.14. The detected masses range from 10^{-18} to 10^{-13} kg and most grains have masses between $3 \cdot 10^{-16}$ and $1 \cdot 10^{-15}$ kg [54].

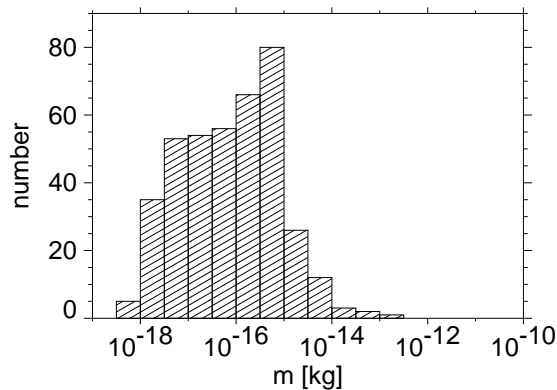


Figure 9.14: Histogram of the mass distribution of interstellar grains detected by the Ulysses dust instrument. The detection threshold for grains impacting with 20 km s^{-1} is $\sim 10^{-18}$ kg.

To compare the in-situ measurements with the mass distribution of dust models based on extinction measurements ([61], MRN distribution hereafter), we calculate the contribution of each logarithmic mass interval to the overall mass density in the interstellar medium. The result is shown in Figure 9.15.

Comparing the in-situ measurements with the MRN distribution one finds two discrepancies:

- Small grains ($m < 10^{-16}$ kg) are deficient.
- The in-situ distribution extends to much larger masses than the MRN cut-off.

The first discrepancy was explained to be caused by the partial removal of small grains due to their interaction with the solar wind magnetic field [24, 53]. In addition,

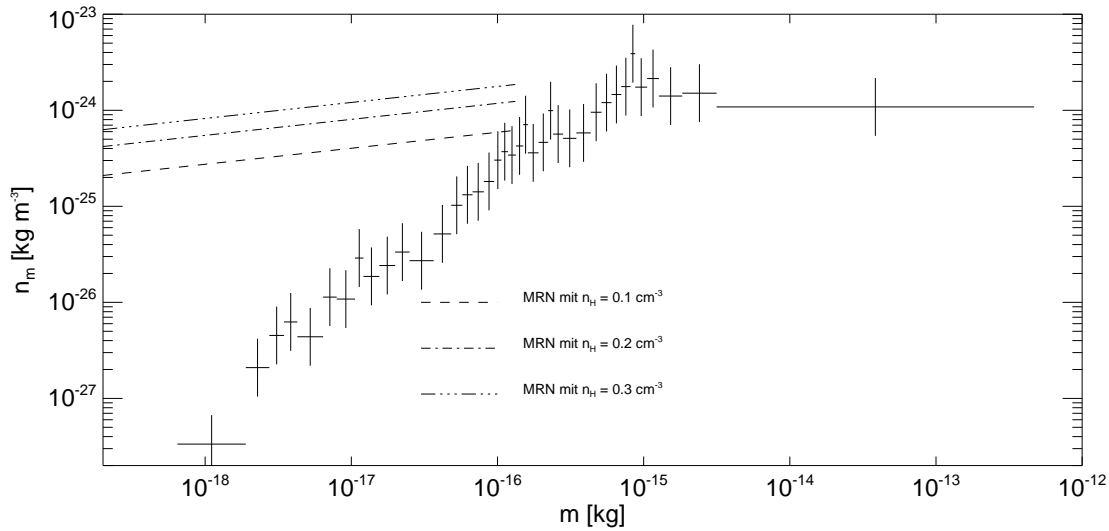


Figure 9.15: Mass density per logarithmic mass interval [13]. Crosses show the distribution of grains detected by Ulysses and Galileo. The broken lines represent the mass per logarithmic mass interval for the MRN distribution assuming three different overall densities of the local interstellar medium (measured by number n_{H} of hydrogen atoms per unit volume). The upper cut-off of the MRN distribution is $2 \cdot 10^{-16}$ kg.

interstellar grains with diameters around $0.4 \mu\text{m}$ are deflected by solar radiation pressure and are thus deficient in the inner solar system [52]. However, as explained above, the existence of *large* interstellar grains cannot be accounted for by dust models based on extinction measurements. Figure 9.15 shows that the large grains detected by Ulysses and Galileo contribute significantly to the overall mass density of heavy elements (heavier than helium) in the local interstellar environment. Calculating the overall mass of the local interstellar medium locked up in grains and assuming that also smaller grains contribute, it was found [13] that dust grains make up 2% of the mass of interstellar matter surrounding the solar system. This is twice the amount of dust expected in the average medium of the Galaxy, which is not expected, since the local medium is less dense than average and already contains large amounts of heavy elements in the gas phase [13].

9.6 Summary and conclusions

The prime goal of the Ulysses mission with respect to dust was to determine the 3-dimensional structure of the interplanetary dust cloud. This goal has been fully accomplished. Ulysses dust data is a crucial ingredient of the comprehensive dynamical model that describes the interplanetary dust cloud [29].

Three more dust populations have been discovered that have not been seen before

by any other in-situ dust experiment: jovian dust stream particles near Jupiter, electromagnetically controlled β -meteoroids above the poles of the Sun, and interstellar grains everywhere else.

The jovian dust streams discovered by Ulysses demonstrated the fact that dust may become an intimate player in magnetospheric processes. We are still at the beginning of our understanding of these interrelations but already now the importance of dust becomes evident. The dust streams are monitors of the volcanic plume activity on Io in a way that is not accomplished yet by any other observational method. So far, only occasional images from Voyagers and Galileo have shown the plumes which are not necessarily related to lava outpours on Io also observed from Earth. Electromagnetically coupled dust grains are probes of the plasma environment in the Io torus where they get their initial charge before they are emitted by Jupiter's magnetic field from the jovian system. Dust stream particles observed at different times originate from different portions of the Io torus. Therefore, observations tracing back to different local times in the Io torus may reveal local time variations in the torus that are predicted by theory. Tiny dust grains can transport material to regions of the magnetosphere where other known magnetospheric processes are unable to transport ions to. Glows of sodium and other elements may be examples for such a transport. Finally, dust stream particles will be used as carriers of information about the chemical composition in Io's volcanic plumes when Cassini flies by Jupiter in December 2000. The dust instrument on board may analyze their chemical composition. In February 2004 Ulysses will fly by Jupiter within a distance of 0.8 AU. A repetition of dust stream measurements in interplanetary space will be beneficial to test our understanding of this new phenomenon.

Yet another population of very small dust particles was observed at high ecliptic latitudes over the Sun's pole. This population has been suggested to be electromagnetically deflected β -meteoroids generated at low ecliptic latitudes and subsequently deflected by the contemporary interplanetary magnetic field to high latitudes. Long-term observations (over two solar cycles) of these particles may prove the prediction that during one solar cycle these particles are found to leave the solar system at high latitudes again while during the other cycle they escape near the ecliptic. This way, these particles are the Sun's analog to Jupiter's dust streams. The study of these particles will provide one further piece in the puzzle of how much dust and from which region in the solar system solid particles are ejected to the interstellar medium.

The question if the interstellar dust grains measured in the solar system by Ulysses and Galileo are "native" to the local interstellar medium, i.e. if they originate from the medium, or if they have been injected, is connected to their kinematic state with respect to the medium. Can we measure a systematic motion of the grains relative to the gas?

The velocity vector of neutral helium atoms with respect to the Sun has been determined with the Ulysses GAS experiment. The helium upstream direction was found to be 252° ecliptic longitude and 5° latitude, and the absolute relative velocity is 25.22 km s^{-1} [72]. By determining the dust upstream direction and comparing it to

the values for the helium atoms, we can establish the kinematic relationship between dust and gas. Since the Ulysses dust detector has a field of view of $\pm 140^\circ$, the impact direction of an individual grain is not accurately determined and we have to apply a statistical analysis of the distribution of measured rotation angles. Figure 9.16 shows the result.

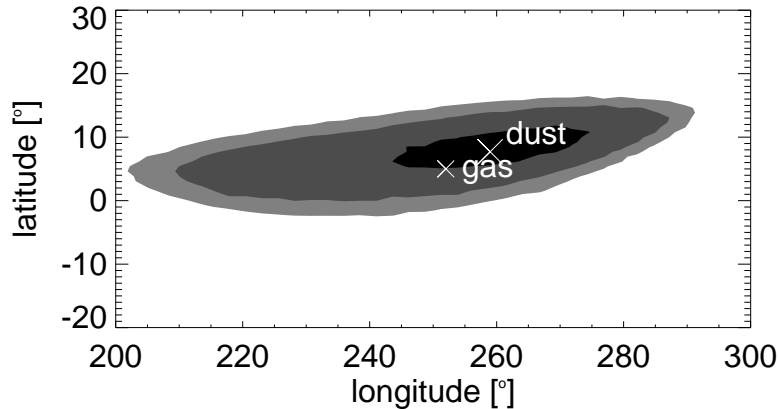


Figure 9.16: Ecliptic longitude and latitude of the upstream direction of interstellar dust grains measured by Ulysses after Jupiter fly-by. The contour plot of a χ^2 analysis shows 1σ , 2σ , and 3σ confidence levels in black, dark grey, and light grey, respectively. The minimum χ^2 is achieved at 259° longitude and 8° latitude (indicated by the cross labeled “dust”). The measurements of the helium upstream direction are indicated by the smaller cross labeled “gas”.

We find that the dust upstream direction coincides with the gas direction on the 1σ confidence level. This indicates, that interstellar gas and dust is in rest with respect to each other. However, since the determination of the dust upstream direction has considerable uncertainties, a velocity dispersion as large as 10 km s^{-1} between dust and gas cannot be ruled out [51]. The Ulysses data indicate a dust component at rest with the local interstellar gas.

For interstellar dust it seems that Ulysses has raised a number of new questions by solving the question about the existence of interstellar dust grains in the solar system. These can be summarized as follows:

- Is the concept of cosmic elementary abundances correct on all length scales or are there small scale inhomogeneities of the galactic chemistry?
- If the answer to the first question is negative, the interstellar grains we measure with Ulysses cannot originate from the interstellar gas of the surrounding medium. So how did they get there and what governs the dynamics of solid grains in the interstellar medium of our Galaxy?

To further confirm our findings and to improve the understanding of the interstellar medium surrounding our solar system, long term measurements are needed because the total flux of interstellar dust grains is low. Ulysses provides an ideal platform for these measurements, because of its fortunate orbit geometry.

Acknowledgements. We thank the ESA/NASA Ulysses projects for effective and successful mission operations. This work has been supported by Deutsches Zentrum für Luft- und Raumfahrt e.V. (DLR) and by the Sonderforschungsbereich Sternentstehung of the Deutsche Forschungsgemeinschaft (DFG).

Bibliography

- [1] **Abraham, P., Leinert, C., Acosta-Pulido, J., Schmidtbreick, L., Lemke, D.**, Zodiacal light observations with ISOPHOT, Proceedings of the conference *The Universe as seen by ISO*, eds. P. Cox and M. F. Kessler, ESA SP-427, 145-148, 1999
- [2] **Abraham, P., Leinert, C. and Lemke, D.**, Interplanetary dust as seen in the zodiacal light with ISO, in *Solid Interstellar Matter: The ISO Revolution*, Les Houches No 11, eds.: L. d'Hendecourt, C. Joblin & A. Jones, EDP Sciences, Les Ullis pp. 3-18, 1999
- [3] **Baguhl, M., Grün, E., Linkert, D., Linkert, G. and Siddique, N.**, Identification of 'small' dust impacts in the Ulysses dust detector data. *Planet. Space Sci.* , **41**, 1085-1098, 1993
- [4] **Baguhl M., D.P. Hamilton, E. Grün, S.F. Dermott, H. Fechtig, M.S. Hanner, J. Kissel, B.A. Lindblad, D. Linkert, G. Linkert, I. Mann, J.A.M. McDonnell, G.E. Morfill, C. Polanskey, R. Riemann, G. Schwehm, P. Staubach and H.A. Zook**, Dust measurements at high ecliptic latitudes, *Science*, **268**, 1016-1019, 1995
- [5] **Baguhl, M., Grün, E., Hamilton, D. P., Linkert, G., Riemann, R., & Staubach, P.**, The flux of interstellar dust observed by Ulysses and Galileo. *Space Science Reviews*, **72**, 471-476, 1995
- [6] **Baguhl, M., Grün, E., & Landgraf, M.** In Situ Measurements of Interstellar Dust with the Ulysses and Galileo Spaceprobes. eds. von Steiger, R., Lallement, R., & Lee, M. A., *The Heliosphere in the Local Interstellar Medium*. Space Science Reviews, Kluwer Academic Publishers, vol. **78**, 165-172, 1996
- [7] **Balogh, A., Erdös, G., Forsyth, R. J. and Smith, E. J.**, The evolution of the interplanetary sector structure in 1992, *Geophys. Res. Lett.*, **20**, 2331-2334, 1993
- [8] **Berg, O. E. and Grün, E.**, Evidence of hyperbolic cosmic dust particles", in: Space Research XIII, Akademie Verlag, Berlin, 1047-1055, 1973

- [9] **Burns, J. A., Lamy, P. L., and Soter, S.**, Radiation forces on small particles in the solar system, *Icarus*, **40**, 1-48, 1979
- [10] **Collins, S. A.**, Spatial color variations in the volcanic plume at Loki on Io, *J. Geophys. Res.*, **86**, 8621, 1981
- [11] **Dermott S.F., Jayaraman S., Xu Y.L., Gustafson B.A.S., and Liou J.C.**, A circumpolar ring of asteroidal dust in resonant lock with the Earth, *Nature*, **369**, 719-723, 1994
- [12] **Divine N.**, Five populations of interplanetary meteoroids, *J. Geophys. Res.*, **98**, 17029-17048, 1993
- [13] **Frisch, P. C., Dorschner, J., Geiß, J., Greenberg, J. M., Grün, E., Landgraf, M., Hoppe, P., Jones, A. P., Krätschmer, W., Linde, T. J., Morfill, G. E., Reach, W., Slavin, J., Svestka, J., Witt, A., & Zank, G. P.** Dust in the Local Interstellar Wind, *Astrophysical Journal*, 525, 492-516, 1999
- [14] **Giese R. H., Kinateder, G., Kneissel, B., Rittich, U.**, Optical models of the three-dimensional distribution of interplanetary dust, in: Properties and interactions of interplanetary dust, eds. R. H. Giese and P. Lamy, Reidel Publishing Co., Dordrecht, 255-259, 1985
- [15] **Giese R. H., Kneissel, B., Rittich, U.**, Three-dimensional zodiacal dust cloud: a comparative study, *Icarus*, **68**, 395-411, 1986
- [16] **Graps, A., Grün, E., Svedhem, H., Krüger, H., Horányi, M., Heck, A., Lammers, S.** Io as a source of the jovian Dust Streams, *Nature*, **405**, 48-50, 2000
- [17] **Grün, E., Pailer, N., Fechtig, H., Kissel, J.**, Orbital and physical characteristics of micrometeoroids in the inner solar system as observed by Helios 1, *Planet. and Space Sci.*, **29**, 333-349, 1980
- [18] **Grün, E. and Zook, H. A.**, Dynamics of micrometeoroids, in: Solid Particles in the Solar System, eds. I. Halliday and B. A. McIntosh, Reidel Publ. Co., Dordrecht, 293-298, 1980
- [19] **Grün, E., Zook, H. A., Fechtig, H., & Giese, R. H.** Collisional balance of the meteoritic complex. *Icarus*, **62**, 244-272, 1985
- [20] **Grün, E., Zook, H.A., Baguhl, M., Fechtig, H., Hanner, M.S., Kissel, J., Lindblad, B.-A., Linkert, D., Linkert, G., Mann, I., McDonnell, J.A.M., Morfill, G.E., Polanskey, C., Riemann, R., Schwehm, G. and Siddique N.**, Ulysses dust measurements near Jupiter. *Science* **257**, 1550-1552, 1992

- [21] Grün, E., Fechtig, H., Giese, R.H., Kissel, J., Linkert, D., Maas, D., McDonnell, J.A.M., Morfill, G.E., Schwehm, G. and Zook, H.A., The Ulysses dust experiment. *Astron. Astrophys. Suppl. Ser.* **92**, 411-423, 1992
- [22] Grün, E., Zook, H. A., Baguhl, M., Balogh, A., Bame, S. J., Fechtig, H., Forsyth, R., Hanner, M. S., Horányi, M., Kissel, J., Lindblad, B.-A., Linkert, D., Linkert, G., Mann, I., McDonnell, J. A. M., Morfill, G. E., Phillips, J. L., Polanskey, C., Schwehm, G., Siddique, N., Staubach, P., Svestka, J., & Taylor, A. Discovery of jovian dust streams and interstellar grains by the Ulysses spacecraft, *Nature*, **362**, 428–430, 1993
- [23] Grün, E., Hamilton, D. P., Baguhl, M., Riemann, R., Horányi, M. and Polanskey, C., Dust streams from comet Shoemaker-Levy 9? *Geophys. Res. Lett.* **21**, 1035-1038, 1994
- [24] Grün, E., Gustafson, B. Å. S., Mann, I., Baguhl, M., Morfill, G. E., Staubach, P., Taylor, A., & Zook, H. A. Interstellar Dust in the Heliosphere. *Astronomy and Astrophysics*, **286**, 915–924, 1994
- [25] Grün, E., Baguhl, M., Fechtig, H., Hamilton, D.P., Kissel, J., Linkert, D., Linkert, G. and Riemann, R., Reduction of Galileo and Ulysses dust data. *Planet. Space Sci.* **43**, 941-951, 1995a
- [26] Grün, E., Baguhl, M., Divine, N., Fechtig, H., Hamilton, D. P., Hanner, M. S., Kissel, J., Lindblad, B.-A., Linkert, D., Linkert, G., Mann, I., McDonnell, J. A. M., Morfill, G. E., Polanskey, C., Riemann, R., Schwehm, G., Siddique, N., Staubach P. and Zook, H. A. Three years of Galileo dust data. *Planet. Space Sci.* **43**, 953-969, 1995b
- [27] Grün, E., Baguhl, M., Divine, N., Fechtig, H., Hamilton, D.P., Hanner, M.S., Kissel, J., Lindblad, B.-A., Linkert, D., Linkert, G., Mann, I., McDonnell, J.A.M., Morfill, G.E., Polanskey, C., Riemann, R., Schwehm, G., Siddique, N., Staubach, P. and Zook, H.A., Two years of Ulysses dust data. *Planet. Space Sci.* **43**, 971-999, 1995c
- [28] Grün, E., Baguhl, M., Hamilton, D. P., Riemann, R., Zook, H. A., Dermott, S., Fechtig, H., Gustafson, B. A., Hanner, M. S., Horányi, M., Khurana, K. K., Kissel, J., Kivelson, M., Lindblad, B.-A., Linkert, D., Linkert, G., Mann, I., McDonnell, J. A. M., Morfill, G. E., Polanskey, C., Schwehm, G. and Srama, R. Constraints from Galileo observations on the origin of jovian dust streams, *Nature* **381**, 395-398, 1996
- [29] Grün, E., Staubach, P., Baguhl, M., Hamilton, D. P., Zook, H. A., Dermott, S., Gustafson, B. A., Fechtig, H., Kissel, J., Linkert, D., Linkert, G., Srama, R., Hanner, M. S., Polanskey, C., Horányi, M., Lindblad, B.-A., Mann, I., McDonnell, J. A. M., Morfill, G. E. and Schwehm, G.

- South-north and radial traverses through the zodiacal cloud. *Icarus*, **129**, 270-288, 1997a
- [30] Grün, E., Krüger, H., Dermott, S., Fechtig, H., Graps, A., Gustafson, B. A., Hamilton, D. P., Hanner, M. S., Heck, A., Horányi, M., Kissel, J., Lindblad, B.-A., Linkert, D., Linkert, G., Mann, I., McDonnell, J. A. M., Morfill, G. E., Polanskey, C., Schwehm, G., Srama, R. and Zook, H. A. Dust measurements in the jovian magnetosphere. *Geophys. Res. Lett.* **24**, 2171-2174, 1997b
- [31] Grün, E., Krüger, H., Graps, A., Hamilton, D. P., Heck, A., Linkert, G., Zook, H. A., Dermott, S., Fechtig, H., Gustafson, B. A., Hanner, M. S., Horányi, M., Kissel, J., Lindblad, B.-A., Linkert, D., Mann, I., McDonnell, J. A. M., Morfill, G. E., Polanskey, C., Schwehm, G., Srama, R., Galileo observes electromagnetically coupled dust in the jovian magnetosphere. *J. Geophys. Res.*, **103**, 20011-20022, 1998
- [32] Gustafson, B.Å. S., & Misconi, N. Y. Streaming of Interstellar Grains in the Solar System, *Nature*, **282**, 276–278, 1979.
- [33] Hamilton, D. P. and Burns, J. A. Ejection of dust from Jupiter's gossamer ring, *Nature* **364**, 695-699, 1993
- [34] Hamilton, D. P., Grün, E., & Baguhl, M., Electromagnetic Escape of Dust from the Solar System. in: Gustafson, B.Å. S., & Hanner, M. S. (eds), *Physics, Chemistry, and Dynamics of Interplanetary Dust*. Astronomical Society of the Pacific Conference Series, vol. **104**, pages 31–34, 1996
- [35] Hanner M. S., Sparrow J. G., Weinberg J. L., and Beeson D. E., Pioneer 10 observations of zodiacal light brightness near the ecliptic: Changes with heliocentric distance, In: Lecture Notes in Physics, **48**: *Interplanetary Dust and Zodiacal Light*, 1976
- [36] Hauser, M.G., Gillett, F.C., Low, F.J., Gautier, T.N., Beichman, C.A., Neugebauer, G., Aumann, H.H., Band, B., Boggess, N., Emerson, J.P., Houck, J.R., Soifer, B.T., and Walker, R.G., IRAS observations of the diffuse infrared background, *Astrophys. J.*, **278**, L15-L18, 1984
- [37] Hauser, M.G., Gautier, T.N., Good, J., and Low, F.J., IRAS observations of the interplanetary dust emission, in *Properties and Interactions of interplanetary dust*, eds. R.H. Giese and P. Lamy, D. Reidel Publ. Co., Dordrecht, pp. 43-48, 1985
- [38] Hoffmann, H.-J., Fechtig, H., Grün, E., Kissel, J., Temporal fluctuation and anisotropy of the micrometeoroid flux in the Earth-Moon system, *Planet. and Space Sci.*, **23**, 985- 991, 1975

- [39] **Holzer, T. E.** Interaction between the Solar Wind and the Interstellar Medium. *Annual Review of Astronomy and Astrophysics*, **27**, 199–234, 1989
- [40] **Horányi, M., Morfill, G.E. and Grün, E.**, Mechanism for the acceleration and ejection of dust grains from Jupiter’s magnetosphere, *Nature* **363**, 144–146, 1993
- [41] **Horányi, M., Morfill, G.E. and Grün, E.**, The Dusty Ballerina Skirt of Jupiter *J. Geophys. Res.* **98**, 21,245–21,251, 1993
- [42] **Horányi, M., Grün, E., Heck, A.** Modeling the Galileo dust measurements at Jupiter. *Geophys. Res. Lett.* **24**, 2175–2178, 1997
- [43] **Humes, D. H., Alvarez, J. M., O’Neal, R.L., Kinard, W. H.**, The interplanetary and near-Jupiter meteoroid environment, *J. Geophys. Res.*, **79**, 3677–3684, 1974
- [44] **Humes, D. H.**, Results of Pioneer 10 and 11 meteoroid experiments: Interplanetary and near-Saturn. *J. Geophys. Res.*, **85**, 5841–5852, 1980
- [45] **Johnson, T. V., Morfill, G., and Grün, E.**, Dust in Jupiter’s magnetosphere: An Io source?, *Geophys. Res. Lett.*, **7**, 305–308, 1980
- [46] **Krüger, H., Grün, E., Graps, A. and Lammers, S.**, Observations of electromagnetically coupled dust in the jovian magnetosphere, *Astrophys. and Space Sci.*, **264**, 247–256, 1999a
- [47] **Krüger, H., Grün, E., Landgraf, M., Baguhl, M., Dermott, S., Fechtig, H., Gustafson, B. A., Hamilton, D. P., Hanner, M. S., Horanyi, M., Kissel, J., Lindblad, B., Linkert, D., Linkert, G., Mann, I., McDonnell, J. A. M., Morfill, G. E., Polanskey, C., Schwehm, G., Srama, R., and Zook, H.**, Three years of Ulysses dust data: 1993 to 1995, *Planetary and Space Science* **47**, 363–383, 1999b
- [48] **Krüger, H., Grün, E., Hamilton, D. P., Baguhl, M., Dermott, S., Fechtig, H., Gustafson, B. A., Hanner, M. S., Horanyi, M., Kissel, J., Lindblad, B. A., Linkert, D., Linkert, G., Mann, I., McDonnell, J. A. M., Morfill, G. E., Polanskey, C., Riemann, R., Schwehm, G., Srama, R., and Zook, H.**, Three years of Galileo dust data: II. 1993 to 1995, *Planetary and Space Science* **47**, 85–106, 1999c
- [49] **Krüger, H., Grün, E., Landgraf, M., Dermott, S., Fechtig, H., Gustafson, B. A., Hamilton, D. P., Hanner, M. S., Horanyi, M., Kissel, J., Lindblad, B., Linkert, D., Linkert, G., Mann, I., McDonnell, J. A. M., Morfill, G. E., Polanskey, C., Schwehm, G., Srama, R., and Zook, H.**, Four years of Ulysses dust data: 1996 to 1999, *Planetary and Space Science*, in preparation, 2001

- [50] **Krüger, H., Grün, E., Graps, A., Bindschadler, D., Dermott, S., Fechtig, H., Gustafson, B. A., Hamilton, D. P., Hanner, M. S., Horanyi, M., Kissel, J., Lindblad, B., Linkert, D., Linkert, G., Mann, I., McDonnell, J. A. M., Morfill, G. E., Polanskey, C., Schwehm, G., Srama, R., and Zook, H.**, One year of Galileo dust data: 1996, *Planetary and Space Science*, in preparation, 2001
- [51] **Landgraf, M.**, Modellierung der Dynamik und Interpretation der In-Situ-Messung interstellaren Staubs in der lokalen Umgebung des Sonnensystems, Ph.D. thesis, Ruprecht-Karls-Universität Heidelberg. (in German), 1998
- [52] **Landgraf, M., Augustsson, K., Grün, E., and Gustafson, B. Å. S.**, Deflection of the Local Interstellar Dust Flow by Solar Radiation Pressure. *Science*, **286**, 2319–2322, 1999
- [53] **Landgraf, M.**, Modeling the Motion and Distribution of Interstellar Dust inside the Heliosphere. *Journal of Geophysical Research*, **105**, **A5**, 10303–10316, 2000
- [54] **Landgraf, M., Baggaley, W. J. and Grün, E.**, Aspects of the Mass Distribution of Interstellar Dust Grains in the Solar System from In-Situ Measurements. *Journal of Geophysical Research*, **105**, **A5**, 10343–10352, 2000
- [55] **Leinert C., Grün, E.**, Interplanetary Dust, in *Physics of the Inner Heliosphere I*. eds. R. Schwenn, and E. Marsch, Springer Verlag, Berlin, pp. 207-275, 1990
- [56] **Leinert C., Richter I., Pitz E., and Planck B.**, The zodiacal light from 1.0 to 0.3 A.U. as observed by the Helios space probes, *Astron. Astrophys.*, **103**, 177-188, 1981
- [57] **Leinert C., Link, H., Pitz, E., and Giese, R.H.**, Interpretation of a rocket photometry of the inner zodiacal light, *Astron. Astrophys.*, **47**, 221-230, 1976
- [58] **Levasseur-Regourd, A.-Ch., and Dumont, R.**, Absolute photometry of zodiacal light, *Astron. Astrophys.*, **84**, 277-279, 1980
- [59] **Levasseur-Regourd, A.-C.** The zodiacal cloud complex, In: Origin and Evolution of interplanetary dust, ed. A. C. Levasseur-Regourd, Kluwer Academic Publishers, Dordrecht, 13-138, 1991
- [60] **Levy, E. H., & Jokipii, J. R.**, Penetration of interstellar dust into the Solar System, *Nature*, **264**, 423–424, 1976
- [61] **Mathis, J. S., Rumpl, W., & Nordsieck, K. H.**, The Size Distribution of Interstellar Grains. *Astrophysical Journal*, **280**, 425, 1997
- [62] **Morfill G. E., and Grün E.**, The motion of charged dust particles in interplanetary space – I. The zodiacal dust cloud, *Planet. Space Sci.* **27**, 1269-1282, 1979

- [63] **Morfill G. E., and Grün E.**, The motion of charged dust particles in interplanetary space – II. Interstellar grains, *Planet. Space Sci.* **27**, 1283-1292, 1979
- [64] **Morfill, G., Grün, E. and Johnson, T. V.**, Dust in Jupiter's magnetosphere: Physical Processes. *Planet. Space Sci.* **28**, 1087-1100, 1980
- [65] **Reach W.T., Franz B.A., Weiland J.L., Hauser M.G., Kelsall T.N., Wright E.L., Rawley G., Stemwedel S.W., and Spiesman W.J.**, Observational confirmation of a circumsolar dust ring by the COBE satellite, *Nature* **374**, 521-523, 1995
- [66] **Scargle, J.D.**, Studies in Astronomical Time Series II.: Statistical Aspects of Spectral Analysis of Unevenly Spaced Data, *Astrophys. J.*, **263**, 835-853, 1982
- [67] **Sekanina, Z. and Southworth, R. B.**, Physical and dynamical studies of meteors, meteor-fragmentation and stream-distribution studies, NASA CR-2615, 1975
- [68] **Spencer, J. R., Sartoretti, P., Bellester, G. E., McEwen, A. S., Clarke, J. T. and McGrath, M. A.**, The Pele plume (Io): observations with the Hubble Space Telescope, *Geophys. Res. Lett.*, **24**, no. **20**, 2471–2474, 1997
- [69] **Staubach P., and E. Grün**, Development of an upgraded meteoroid model, *Advances in Space Res.*, **16**, (11)103-(11)106, 1995
- [70] **Staubach, P.**, Numerische Modellierung der Dynamik von Mikrometeoroiden und ihre Bedeutung für interplanetare Raumsonden und geozentrische Satelliten, PhD. thesis, Ruprecht-Karls-Universität Heidelberg (in German), 1996
- [71] **Wehry, A. and Mann, I.**, Identification of β -meteoroids from measurements of the dust detector on board the Ulysses spacecraft, *Astron. & Astrophys.*, **341**, 296, 1999
- [72] **Witte, M., Rosenbauer, H., Banaszekiewicz, H., & Fahr, H.** The Ulysses neutral gas experiment - Determination of the velocity and temperature of the interstellar neutral helium. *Advances in Space Res.*, **13**, (6)121–(6)130, 1993
- [73] **Zook, H. A. and Berg, O. E.**, A source for hyperbolic cosmic dust particles, *Planet. and Space Sci.*, **23**, 183-203, 1975
- [74] **Zook, H. A., Grün, E., Baguhl, M., Hamilton, D. P., Linkert, G., Liou, J.-C., Forsyth, R. and Phillips, J. L.**, Solar wind magnetic field bending of jovian dust trajectories, *Science* **274**, 1501-1503, 1996